

Study of aerosol optical properties in Lumbini, Nepal

Santosh Sapkota¹, Sabin Gautam², Santosh Pokhrel¹
Aayush Gautam³, Kailash Basnet¹, Roshan Kumar Mishra⁴, Jeevan Regmi^{1,*}

¹Prithvi Narayan Campus, Tribhuvan University

²Pokhara Astronomical Society

³Birendra Multiple Campus, Tribhuvan University

⁴University of Maryland, Baltimore County

*Corresponding author. Email: jsregmi28@gmail.com

Abstract

The mixture of different sized particles (fine and coarse) with air composition forms aerosols. Increased economic activities, vehicles, and rapid urbanization made Lumbini one of the heavily polluted regions in Nepal. Data are extracted from AERONET websites between 2013 to 2019 with standard deviation. We are mainly focused on understanding variations in aerosol optical properties: aerosol optical depth (AOD), angstrom parameter (α and β), visibility, single-scattering albedo (SSA), refractive index (real and imaginary), and asymmetry parameter (AP) in the Lumbini region. The maximum value of AOD (675nm) in Lumbini occurred mostly during post-monsoon season (0.61 ± 0.38) whereas; the values of AOD were found to be lower during the monsoon season (0.18 ± 0.12). Most of the AOD values except monsoon season are found to be greater than 0.4, indicating a higher level of pollution in the study area. There is a weak correlation between precipitable water and AOD, maximum correlation (0.04) occurs at the lowest value of AOD at 440nm while the minimum (0.01) at the highest value of AOD at 1020nm. The turbidity coefficient (β) has an adverse effect on visibility. The average Visibility over Lumbini was found to be 8.76 ± 4.95 km during the period of 2013-2019. Single-scattering albedo (SSA) accretions occur at wavelengths between 440 and 675 nm, but the pattern changes from 675 nm to 1020 nm. All parameters were found to be distinct and seasonal fluctuations among this station are mainly due to the different aerosols availability such as biomass burning, mixed aerosols, and anthropogenic aerosols over the Lumbini site.

Keywords

Aerosol optical depth, Angstrom exponent, Lumbini.

Article information

Manuscript received: October 09, 2022; Accepted: March 18, 2023

DOI <https://doi.org/10.3126/bibechana.v20i1.48825>

This work is licensed under the Creative Commons CC BY-NC License. <https://creativecommons.org/licenses/by-nc/4.0/>

1 Introduction

Aerosols are atmospheric molecules that are either produced by anthropogenic factors (fossil fuel, burning, biomass, transportation, etc.) or by nat-

ural factors (volcanic, sea salt, desert, etc.). It has a variety of potential effects on our planet's radiation balance. Aerosols can absorb and scatter solar

energy, which has an impact on cloud formation by changing the microphysics and lifetime of the clouds [1]. Though a lot of information about our climate system is known, there are more parameters and associated factors that make a deep understanding of the climate system uncertain [2]. Aerosols in the atmosphere are responsible for changing the climate system, reducing visibility and crop productivity, and harming human health [3]. The size and structure of aerosols vary from location to location and are influenced by pollution levels that make their optical and microphysical properties complicated [4]. Studies on aerosols conducted in the past have also shown that aerosols produced by human activity can change regional temperature, the hydrological cycle, clouds, and precipitation [5]. The main difficulty in the current climatic study is to quantify regional-scale variations in aerosol concentration, composition, and size with high enough temporal and geographical resolution [6], which necessitates methods that integrate observations with atmospheric models.

The combination of anthropogenic sources, and biomass burning over the IGP region, which also affects the air quality in Lumbini, is the main source of aerosol loading [7], which results in the creation of atmospheric black carbon (ABC) [8–10]. Thus, emitted particles get trapped under conducive meteorological conditions which results in the air pollution of the region [11].

Several parameters, including Aerosol Optical Depth (AOD), Angstrom Exponent (α), Turbidity Coefficient (β), Precipitable Water (PW), Single Scattering Albedo (SSA), visibility and Asymmetry Parameter (AP) has been examined in this article. SSA represents the scattering ability of the aerosol; higher SSA values denote a more scattering aerosol, while lower SSA values indicate absorbing aerosol. By analyzing SSA values, we can predict whether the aerosols have cooling or warming effect [12]. For purely scattering aerosol, the value of SSA is 1 and for pure absorbing particles, it is zero. The Value of the SSA varies with the aerosol types also. For example; the value of SSA for biomass burning ranges from 0.88-0.94, for desert dust it ranges from 0.92-0.99 and it is 0.89-0.98 for urban industrial aerosol [13].

The real and imaginary parts, which make up the refractive index, are adversely influence by chemical composition [14]. The refractive index describes how atmospheric particles scatter and absorb light [15]. The real part's higher value indicates the domination of scattering type of aerosol particles, whereas the imaginary part's higher value shows the domination of absorbing type of aerosol particles.

Various kinds of aerosols, the refractive index's real value has a range of possible values. The value

of the imaginary part varies from 0.003-0.014 for urban industrial aerosols, 0.00093-0.021 for biomass burning, and 0.007-0.0029 for desert dust, and the value of real part ranges from 1.40-1.47 for urban industrial aerosols, 1.47-1.52 for biomass burning, and 1.36-1.56 for desert dust [16].

The Asymmetry Parameter (ASY), which is affected by particle size and composition, has a value between -1 (backscattered) and 1 (forward scattered) [17]. The dependence of aerosol loading on a particular size is explained by the relationship of AOD and Angstrom exponents. The Turbidity Coefficient (β) reflects aerosol loading, whereas the Angstrom exponent (α) denotes aerosol size distribution. The variation in the size of aerosol has guided by its source.

The aerosol optical depth (AOD) is an extinction coefficient of aerosols in the vertical direction, and it is used to describe turbidity, estimate the aerosol content of the atmosphere, evaluate the degree of atmospheric environmental pollution, and can be measured to assess the aerosol load on the atmosphere. Moreover, the amount of water that comes back to the earth's surface in the form of precipitation when the cloud condenses formed by evaporation from the surface of the earth is known as precipitable water. It is the main component of the greenhouse because it is capable of absorbing and reemitting infrared radiation. This work mainly focuses on understanding the aerosol optical properties over Lumbini on monthly variation and also describes the seasonal variation.

2 Data set and Methodology

This research is focused on the various aerosol properties over Lumbini, Nepal (27.67N, 83.50E, 150m elevation). Lumbini is known as the birthplace of the Buddha, which is located within the Nepal terai region, called the land of the subtropical chain of forests marshes, and grasses. Lumbini is one of Asia's most polluted regions in the Terai region [18]. The major sources of air pollution are gases produced by different industries, brick-kiln, fire, and smoke. Besides this, Lumbini is bordered by India and lies in the IGP region, so the transportation of various types of air pollutants from the northern part of India leads to an increase in the air pollution over Lumbini [19]. Since Lumbini represents the characteristics of the Terai region of Nepal bordered to India especially, IGP region and a historical Pilgrimage site of Nepal, we are motivated to study the various aspects of aerosol optical properties.

Aeronet Robotics network (AERONET) (aeronet.gsfc.nasa.gov) has installed the Cimel Sun-Photometer in Lumbini International Research Institute (LIRI). We have used AERONET level 2,

version 3 data for our analysis which are quality assured data of Lumbini site over the period of 7 years from January 2013 to December 2019 [20].

There are eight distinct ways to measure AOD using a solar photometer, with wavelengths ranging from 340 nm to 1020nm [21]. The relationship between AOD and angstrom exponent (α) is given by the power-law equation [22]

$$\tau = \beta\lambda^{-\alpha} \quad (1)$$

The wavelength in microns associated with AOD value is denoted by λ . Angstrom's turbidity coefficient is denoted by β . Equation (1) can be written in the logarithmic format as:

$$\ln \tau(\lambda) = \ln \beta - \alpha \ln \lambda \quad (2)$$

Ångström parameters (α and β) were obtained from equation (2). From the spectral AOD (λ), the angstrom exponent (AE) α can be further defined as:

$$\alpha = -\frac{d \ln \tau AOD(\lambda)}{d \ln \lambda} = \frac{\ln \frac{\tau AOD \lambda_2}{\tau AOD \lambda_1}}{\ln \frac{\lambda_2}{\lambda_1}} \quad (3)$$

The visibility (V) of the air in km is given by the following formula [23].

$$\beta = 0.5\alpha \left(\frac{3.912}{V} - 0.01162 \right) (0.02472V(V-5) + 1.132) \quad (4)$$

where V denotes the visibility in the atmosphere which is inversely proportional to extinction coefficient, [24].

The ratio of scattering coefficient to the extinction coefficient gives the single scattering albedo (SSA), can be expressed as:

$$\omega = \frac{\sigma_{scatt}}{\sigma} \quad (5)$$

The asymmetry parameter can be calculated as,

$$g = \frac{1}{2} \int_0^\pi \cos \theta' P(\theta), \sin \theta, d\theta \quad (6)$$

where, θ angle between incident and scattering direction. $P(\theta)$ represents the angular distribution of scattering light.

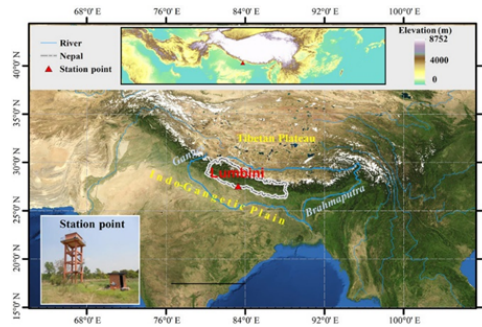


Figure 1: Map showing the geographical location of Lumbini, Nepal.

3 Results and Discussion

To acquire a qualitative knowledge of atmospheric aerosols and aerosol size, the AOD and Angstrom exponent (α) are often used. The parameter with low and high values indicates coarse and fine particle dominance, respectively. Figure 2 shows the monthly average aerosol optical properties, namely, AOD, Angstrom exponent (AE) (440-870nm), and PW from January to December at Lumbini with standard deviations from 2013 to 2019. The monthly average is obtained by averaging daily mean data over seven years.

The highest AOD (675nm) was found in the monsoon season in June (0.61 ± 0.38). Due to fog, haze, and clouds, the AOD is higher during the winter and post-monsoon seasons [25]. In contrast to the pre-monsoon and summer seasons, it was determined that the angstrom exponent (α) was at its

maximum during the post-monsoon and winter seasons due to the influence of anthropogenic sources.

The value of α was found to be greater than 1.0 in all months of the year, representing the dominance of fine mode aerosols due to combustion related anthropogenic sources. The lowest AOD was found in the monsoon season in July (0.21 ± 0.14) due to the increment in the level of precipitable water that helps to wash out the aerosols in the atmosphere.

The amount of precipitable water was shown to rise to start in January (1.23 ± 0.23), reach its peak in July (5.91 ± 0.36), and then gradually decline. In the Lumbini site, the monsoon represents the rainy season and is responsible for 75 % of the annual precipitable water. The variation of AOD, α , and precipitable water was found to be similar to [26], which agrees with our results.

The short wavelength dominates the fine-mode

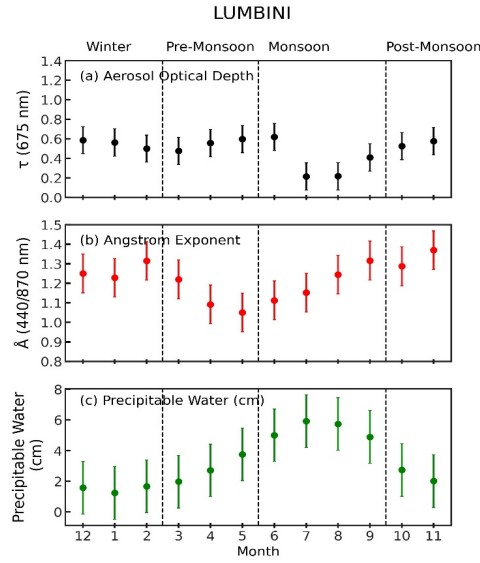


Figure 2: AERONET station Lumbini monthly averages of AOD (440nm), Angstrom exponent (440-870nm), and Precipitable water.

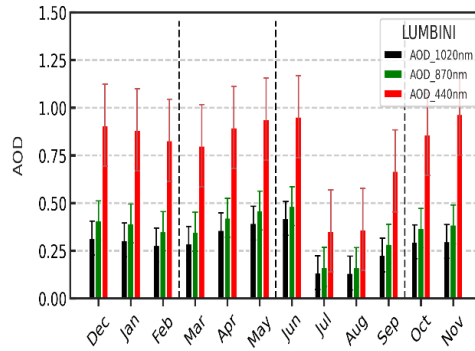


Figure 3: Monthly average AOD observed between January 2013 and December 2019 using AERONET sun/sky radiometers at 1020, 870, and 440 nm.

particles at wavelengths below 870 nm, whereas the long wavelength dominates the coarse-mode particles at wavelengths over 870 nm. AODs first show considerable seasonal and wavelength dependence. As wavelength rises, AODs eventually decrease, as shown in Fig. 3. The abundance of smaller size particles is indicated by higher AODs at lower wavelengths.

AODs with wavelengths of (1020 nm, 870 nm, and 440 nm) and precipitable water (cm) at the Lumbini station have very weak correlation coefficients of 0.01, 0.02, and 0.04 correspondingly, indicating the weak correlation represented in Fig. 4. The fact that there is a weak correlation between AOD's of various wavelengths and precipitable water suggests the amount of aerosol or other particulate matter in the atmosphere decreases as precipitable water increases. The correlation coefficient was found to be higher at the lowest wavelength 440 nm with perceptible water in comparison with 870 and 1020nm. The linear regression functions of

the daily AOD concentration (y) with the perceptible water(x) were $y = -0.01x + 0.34(R^2 = 0.01)$ at 1020nm

$y = -0.02x + 0.43(R^2 = 0.02)$ at 870nm, and

$y = -0.06x + 0.99(R^2 = 0.04)$ at 440nm.

The Turbidity Coefficient (β) is strongly linked with visibility impairment. A measure of the quantity of aerosol loading in the atmosphere is the turbidity coefficient. The relationship between visibility and the turbidity coefficient (α) is inverse (Fig.5), indicating that visibility is affected by aerosol loading to some extent. The average visibility for the given period of time was found to be 8.76 ± 4.95 km which is significantly low and indicates Lumbini having a hazy atmosphere most of the time. But few monsoon days are fairly clean with the highest visibility in July (20 km) and August (19 km). Because more precipitable water washes out the aerosol load in the atmosphere during the monsoon season, visibility was found to be at its maximum. Winter, post-monsoon, and pre-

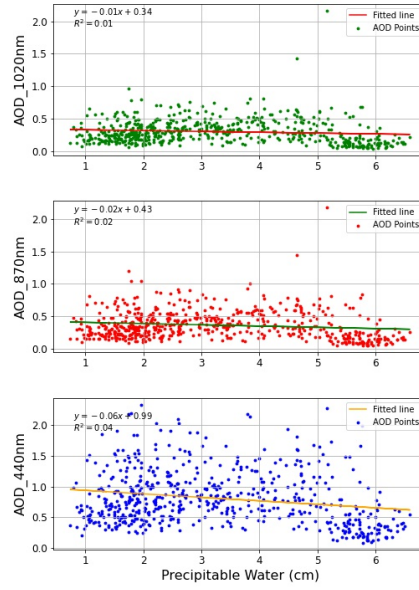


Figure 4: Correlation between Precipitable Water and AODs (1020, 870 and 440nm) of Lumbini locations of Nepal.

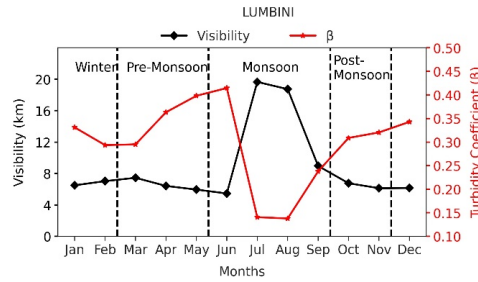


Figure 5: Relation between visibility and Turbidity coefficient (β) over Lumbini from 2013 to 2019.

monsoon seasons have the lowest visibility due to Fog, haze, cold waves, and smoke from industries. At the Lumbini station, the turbidity coefficient value was determined to be higher than 0.15, indicating a turbid atmosphere at all seasons.

Single Scattering albedo (SSA), a metric of light extinction, is another important optical property of aerosols to make sure the aerosol's scattering and absorption properties, which are strongly dependent on wavelength and have significant characteristics over Lumbini. Single scattering albedo (SSA) is calculated using the particle scattering coefficient to total extinction coefficient ratio [27]. The chemical nature and size distribution of aerosols have a significant impact on SSA [28]. Pure absorption has a value of zero, while scattering has a value of one [29, 30].

The reported SSA estimates for desert dust (0.78-0.94), urban and mixed aerosols (0.83-0.98),

and biomass burning (0.92-0.99) [28]. The average SSA shows high wavelength dependence, increasing from 0.90 ± 0.03 at 440nm to 0.92 ± 0.03 at 675nm and dropping to 0.90 ± 0.04 at 1020nm (Fig.6). The monsoon and post-monsoon seasons, respectively, have seen the highest and lowest SSA levels. The highest SSA value indicates that scattering aerosols predominate, whereas the lowest SSA value indicates that light-absorbing aerosols predominate. Our values are supported by earlier research [29] that indicates the summer and post-monsoon seasons experienced the largest and least SSA, respectively. Over Lumbini, post-monsoon had the highest concentration of light-absorbing aerosols compared to other seasons [30].

Similar trend of spectral variation of SSA was observed in Pokhara [31]. The real and imaginary parts of the refractive index at the Lumbini location are depicted in Fig. 7. At 440 nm, the average real

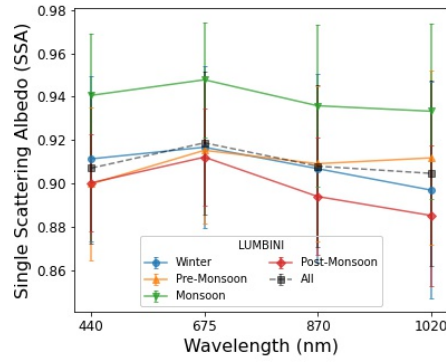


Figure 6: Seasonal variation of SSA over Lumbini from 2013 to 2019.

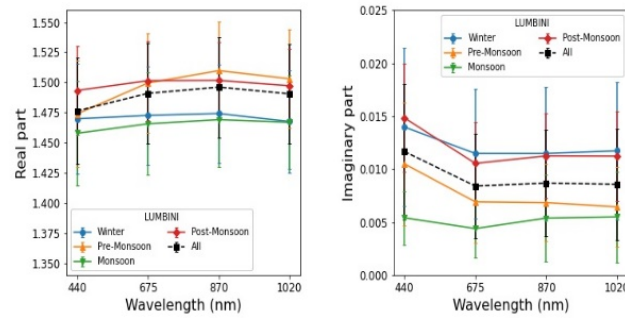


Figure 7: Seasonal variation of the aerosol real and imaginary part of the refractive index over Lumbini from 2013 to 2019.

part of the refractive index is 1.47 ± 0.04 ; at 870 nm, it is 1.49 ± 0.04 ; and at 1020 nm, it is 1.48 ± 0.04 . The real part of the refractive index reaches its maximum and minimum values during the post-monsoon and monsoon seasons, respectively, which agrees with the possible range of values as given by [27] for various types of aerosol particles and previous result for the Lumbini region [26]. The hygroscopic growth of aerosol and relative humidity are responsible for the decrease in the value of the refractive index (real part) during the monsoon season. Additionally, the average imaginary part of the refractive index declines from 0.01 ± 0.006 at 440 nm to 0.008 ± 0.004 at 675 nm and then remains almost constant at 870 nm and 1020 nm. In contrast to the monsoon and pre-monsoon seasons, the post-monsoon and winter seasons were shown to have greater values for the imaginary part of the refractive index.

The value of the asymmetry parameter has found to be wavelength dependent. As the wavelength rises, the value of the asymmetry parameter (g) falls (Fig. 8). The average value of the asymmetry parameter (g) decreases from 0.72 ± 0.02 at 440 nm to 0.64 ± 0.03 at 1020nm. The value gradually declines from 440 nm to 1020 nm during the winter, post-monsoon, and monsoon seasons while

during pre-monsoon the value increases from 870nm to 1020 nm.

4 Conclusion

The key aerosol optical properties like AOD, AE, PW, SSA, AP and refractive index over Lumbini site was analyzed from 2013 to 2019 using AERONET data. It revealed some interesting features. The months of December and July were found to have the highest monthly average AOD (675nm). The alpha value was found to be more than 1.0, indicating that fine mode aerosols predominated throughout the duration of a year. 75 % of the water vapour that is observable throughout the year is precipitable during the monsoon season. AOD values are found to be spectral dependent. It is observed that AOD value decreases with the increase in wavelength. AODs of short wavelengths can give higher precision in measuring the size of aerosols. This implies that the aerosols' size is dispersed in the atmosphere. The Precipitable Water observed higher during the periods when the AOD is also higher indicating the possibility of the hygroscopic growth of aerosols and the dust storm from IGP region. The visibility and the turbidity coefficient (β) have an inverse relation-

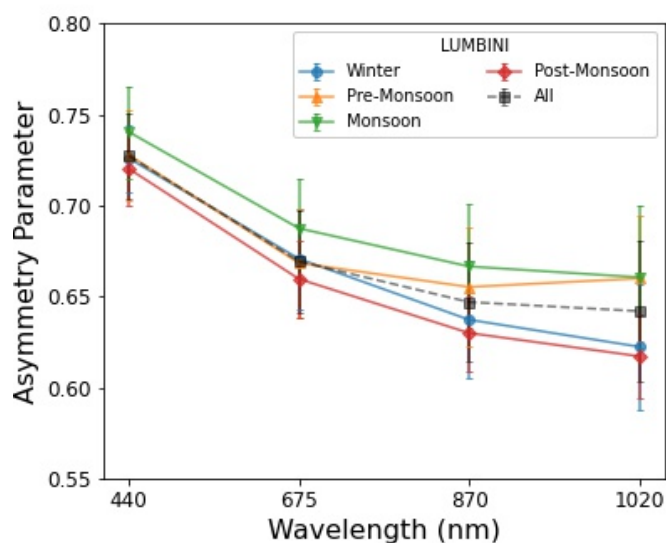


Figure 8: Seasonal variation of the asymmetry parameter over Lumbini from 2013 to 2019.

ship. Due to more precipitable water during summer, the visibility over Lumbini was greater during the period of highest precipitable water. The average SSA value of different years for Lumbini increases progressively from 440 nm to 675 nm and shows a different pattern from 675nm to 1020nm. The SSA value is significantly greater during the monsoon, indicating that there is much more scattering of aerosol during the summer season, but the SSA was lowest during the post-monsoon season. Seasonal variations in spectral SSA levels were observed. The asymmetry parameter and refractive index (RI) were found to be wavelength dependent in the range of 440–1020 nm. Aerosols from biomass burning, mixed aerosols, and anthropogenic aerosols all have an impact on the Lumbini site.

References

- [1] D. Boucher, O. and Randall, C. Artaxo, P. and Bretherton, G. Feingold, and X. Y. Forster, P. and Zhang. Clouds and aerosols in climate change 2013: the physical science basis. contribution of working group i to the fifth assessment report of the intergovernmental panel on climate change. Technical report, Cambridge University Press, 2013.
- [2] T. F. Stocker, D. Qin, G. K. Plattner, M. M. Tignor, Boschung J. Allen, S. K., and P. M. Midgley. Climate change 2013: The physical science basis. contribution of working group i to the fifth assessment report of ipcc the intergovernmental panel on climate change. Technical report, IPCC, 2014.
- [3] G. Ramanathan, V. and Carmichael. Global and regional climate changes due to black carbon. *Nat. Geosci.*, 10(1):221–227, 2008. [10.1038/ngeo156](https://doi.org/10.1038/ngeo156)
- [4] S. and Devara P.C.S. and Bisht D.S. and Srivastava M.K. and Tripathi S.N. and Goloub P. and Holben B.N. Srivastava, A.K. and Tiwari. Pre-monsoon aerosol characteristics over the indo-gangetic basin: implications to climatic impact. *Annales Geophysicae*, 29:789–804, 2011.
- [5] V. C. P. J. Ramanathan, P. J. Crutzen, J. T. Kiehl, and D. Rosenfeld. Aerosols, climate, and the hydrological cycle. *Annales Geophysicae*, 294:2119–2124, 2001. [10.1126/science.1064034](https://doi.org/10.1126/science.1064034)
- [6] R. and Ali S. and Ajmal M. and Khan G. Alam, K. and Khan, W. Muhammad, and M. A. Ali. Variability of aerosol optical depth over swat in northern pakistan based on satellite data. *Arabian Journal of Geosciences*, 8:547–555, 2015. [10.1007/s12517-013-1237-2](https://doi.org/10.1007/s12517-013-1237-2)
- [7] S. Rupakheti, D. and Kang and M. Rupakheti. Two heavy haze events over lumbini in southern nepal: Enhanced aerosol radiative forcing and heating rates. *Arabian Journal of Geosciences*, 236:117658, 2020. [10.1016/j.atmosenv.2020.117658](https://doi.org/10.1016/j.atmosenv.2020.117658)
- [8] P. J. Ramanathan, V. and Crutzen. Two heavy haze events over lumbini in southern nepal:

[10.1017/CBO9781107415324](https://doi.org/10.1017/CBO9781107415324)

- Enhanced aerosol radiative forcing and heating rates. *Atmospheric Environment*, 37:4033–4035, 1994.
- [9] K. Ram and M. M. Sarin. Day–night variability of ec, oc, wsoc and inorganic ions in urban environment of indo-gangetic plain: implications to secondary aerosol formation. *Atmospheric Environment*, 45:460–468, 2011. [10.1016/j.atmosenv.2010.09.055](https://doi.org/10.1016/j.atmosenv.2010.09.055)
- [10] K. Ram and M. M. Sarin. Atmospheric carbonaceous aerosols from indo-gangetic plain and central himalaya: Impact of anthropogenic sources. *Journal of Environmental Management*, 148:153–163, 2015. [0.1016/j.jenvman.2014.08.015](https://doi.org/10.1016/j.jenvman.2014.08.015)
- [11] T. F. Slutsker Holben, B. N. and Eck, J. P. and Setzer A. I. A., Tanre D. and Buis, and A. Smirnov. Eronet—a federated instrument network and data archive for aerosol characterization. *Journal of Environmental Management*, 66:1–16, 1998. [10.1016/S0034-4257\(98\)00031-5](https://doi.org/10.1016/S0034-4257(98)00031-5)
- [12] J. M. Haywood and K. P. Shine. The effect of anthropogenic sulfate and soot aerosol on the clear sky planetary radiation budget. *Geophysical Research Letters*, 22:601–606, 1995. [10.1029/95GL00075](https://doi.org/10.1029/95GL00075)
- [13] O. Dubovik, B. Holben, A. Eck, T. F. and Smirnov, Y. J. Kaufman, and I. King, M. D. and Slutsker. Variability of absorption and optical properties of key aerosol types observed in worldwide locations. *Geophysical Research Letters*, 59(3):590–608, 2002.
- [14] H. Bibi, K. Alam, T. Blaschke, S. Bibi, and M. J. Iqbal. Long-term (2007–2013) analysis of aerosol optical properties over four locations in the indo-gangetic plains. *Geophysical Research Letters*, 55(23):6199–6211, 2016. [10.1364/AO.55.006199](https://doi.org/10.1364/AO.55.006199)
- [15] A. J. Adesina, K. R. Kumar, V. Sivakumar, and D. Griffith. Direct radiative forcing of urban aerosols over pretoria (25.75 s, 28.28 e) using aeronet sunphotometer data: First scientific results and environmental impact. *Journal of Environmental Sciences*, 26(21):2459–2474, 2014. [10.1016/j.jes.2014.04.006](https://doi.org/10.1016/j.jes.2014.04.006)
- [16] O. Dubovik, B. Holben, T. F. Eck, A. Smirnov, Y. J. Kaufman, M. D. King, and I. Slutsker. Variability of absorption and optical properties of key aerosol types observed in worldwide locations. *Journal of the Atmospheric Sciences*, 59(3):590–608, 2002.
- [17] T. F. Eck, B. N. Holben, O. Dubovik, A. Smirnov, P. Goloub, and I. Chen, H. B. and Slutsker. Columnar aerosol optical properties at aeronet sites in central eastern asia and aerosol transport to the tropical mid-pacific. *Journal of the Atmospheric Sciences*, 110(D6), 2005. [10.1029/2004JD005274](https://doi.org/10.1029/2004JD005274)
- [18] D. Rupakheti, S. Kang, and M. Rupakheti. Two heavy haze events over lumbini in southern nepal: Enhanced aerosol radiative forcing and heating rates. *Atmospheric Environment*, 236:117658, 2020. [10.1016/j.atmosenv.2020.117658](https://doi.org/10.1016/j.atmosenv.2020.117658)
- [19] H. Koschmieder. Theorie der horizontalen sichtweite. *Beitrage zur Physik der freien Atmosphere*, 174:33–53, 1924.
- [20] M. Wrensch, R. B. Jenkins, J. S. Chang, R. F. Yeh, Y. Xiao, Decker, and J. K. P. A. and Wiencke. Variants in the cdkn2b and rtel1 regions are associated with high-grade glioma susceptibility. *Nature Genetics*, 141(8):905–908, 2009.
- [21] B. N. Holben, T. F. Eck, I. A. Slutsker, D. Tanre, J. P. Buis, Setzer, and A. Smirnov. Aeronet—a federated instrument network and data archive for aerosol characterization. *Remote Sensing of Environment*, 66(1):1–16, 1998. [10.1016/S0034-4257\(98\)00031-5](https://doi.org/10.1016/S0034-4257(98)00031-5)
- [22] A. Ångström. Techniques of determining the turbidity of the atmosphere. *Tellus*, 13(2):214–223, 1961. [10.3402/tellusa.v13i2.9493](https://doi.org/10.3402/tellusa.v13i2.9493)
- [23] M. Iqbal. An introduction to solar radiation. *Elsevier*, 2002.
- [24] H. Koschmieder. Theorie der horizontalen sichtweite. *Beitrage zur Physik der freien Atmosphere*, pages 33–53, 1924.
- [25] M. Kumar, S. Tiwari, V. Murari, A. K. Singh, and T. Banerjee. Wintertime characteristics of aerosols at middle indo-gangetic plain: Impacts of regional meteorology and long range transport. *Atmospheric Environment*, 104:162–175, 2015. [10.1016/j.atmosenv.2015.01.014](https://doi.org/10.1016/j.atmosenv.2015.01.014)
- [26] D. Rupakheti, S. Kang, M. Rupakheti, Z. Cong, L. Tripathi, Panday, A. K., and B. N. Holben. Observation of optical properties and sources of aerosols at buddha’s birthplace, lumbini, nepal: environmental implications. *Environmental Science and Pollution Research*, 25(15):14868–14881, 2018. [10.1007/s11356-018-1713-z27](https://doi.org/10.1007/s11356-018-1713-z27)

- [27] H. Bibi, K. Alam, T. Blaschke, S. Bibi, and M. J. Iqbal. Long-term (2007–2013) analysis of aerosol optical properties over four locations in the indo-gangetic plains. *Applied Optics*, 55(23):6199–6211, 2016.
- [28] O. Dubovik, B. Holben, T. F. Eck, A. Smirnov, Kaufman Y. J., M. D. King, and I. Slutsker. Variability of absorption and optical properties of key aerosol types observed in worldwide locations. *Journal of the Atmospheric Sciences*, 59(3):590–608, 2002. [10.1364/AO.55.006199](https://doi.org/10.1364/AO.55.006199)
- [29] C. Bohren, D. Huffman, and Z. amp; amp; Kam. Book-review-absorption and scattering of light by small particles. *Nature*, 306(5943):625, 1983.
- [30] O. Dubovik, B. Holben, T. F. Eck, A. Smirnov, Y. J. Kaufman, M. D. King, and I. Slutsker. Variability of absorption and optical properties of key aerosol types observed in worldwide locations. *Journal of the Atmospheric Sciences*, 59(3):590–608, 2002.
- [31] J. Regmi, K. N. Poudyal, A. Pokhrel, M. Gyawali, L. Tripathee, A. Panday, and R. Aryal. Investigation of aerosol climatology and long-range transport of aerosols over pokhara, nepal. *Atmosphere*, 11(8):874, 2020.